Journal of Optoelectronics and Advanced Materials Vol. 5, No. 4, December 2003, p. 977 - 983

COMPARISON BETWEEN EFFECTS OF PRESSURE ON SPIN TRANSITION COMPOUNDS AND PRUSSIAN BLUE ANALOGUES

A. Sava[ab*], C. Enachescu[ab], A. Stancu[a], K. Boukheddaden[b], E. Codjovi[b], I. Maurin[b], F. Varret[b]

[a]"Alexandru Ioan Cuza" University, Faculty of Physics, Iasi 6600, Romania
[b]Laboratoire de Magnétisme et d'Optique, CNRS-UMR 8634, F78035 Versailles Cédex, France

The behaviour of two types of photo-excitable, bistable systems under the influence of pressure have been investigated. A comparison was madebetween Prussian blue analogues and a much more studied class of compounds: spin transition compounds. The experiments have been carried out with a helium-gas-pressure apparatus with optical-reflectivity detection. The thermal hysteresis loops of these two kinds of compounds have been recorded under the influence of pressure. The phase diagrams in (p, T) axis have been determined and discussed.

(Received July 14, 2003; accepted August 21, 2003)

Keywords: Spin transition, Prussian blue analogues, Thermal hysteresis, Pressure effect

1. Introduction

Molecular complexes containing $3d^4$-$3d^7$ metal ions in octahedral surroundings are bistable systems. They have a high spin (HS) or a low spin (LS) state according to the ligand field strength. So, if one considers this ligand field strength, Δ, and compares with the coupling energy of the electrons, Π, there are three possibilities: i). $\Delta >> \Pi$, electrons tend to occupy orbitals with lower energy, violating Hund's rule and in this case one obtains a minimum of the total spin and says that the ion is in the low spin state (LS) ; ii). $\Delta << \Pi$, electrons will occupy a number of orbitals as large as possible, in accordance with Hund's rule and in this case one says that the ion is in the high spin state (HS); iii). the most interesting case: $\Delta \sim \Pi$, when it is possible that the ion to pass from one state to another under the effect of an external perturbation: variation of light, temperature or pressure. These compounds are known as spin-crossover or spin-transition compounds [1]. Their bistability, originating from intra-molecular vibronic coupling, can be enhanced by intermolecular interactions, which are elastic in nature, and these may introduce a first-order transition with thermal hysteresis loop. The width of the loop depends on the strength of the coupling. Due to their bistable character, these systems are potential candidates for information storage applications [2].

From the experimental point of view many studies have been carried out, because the spin transition is accompanied by the change of magnetization state (from LS diamagnetic state to a HS paramagnetic one), the change of color (from red-purple LS state to white-transparent HS), and the change in volume, around 10% from initial state [3-5].

Another class of studied compounds are the Prussian blue analogues (PBA). The synthesis of the powdered samples involves substitution reactions of the water molecules of the hexaaqua complex $[Co^{II}(H_2O)_6]^{2+}$ by $[Fe^{III}(CN)_6]^{3-}$. The goal is a progressive increase of the cobalt ligand field as oxygen atoms from water are replaced by nitrogen from cyanides. For a sufficient number of nitrogen atoms around the cobalt ion, it becomes low spin. Then, a chemically induced electron transfer leads

---

[*] Corresponding author: ancasava@yahoo.com

spontaneously to more stable diamagnetic Co(III)-Fe(II) pairs. Once the diamagnetic pairs are obtained, the photo induced electron transfer should occur, leading to paramagnetic Co(II)-Fe(III) pairs [6]. XANES (X-ray Absorption Near Edge Spectroscopy) measurements, Infrared Spectroscopy and X-ary Powder Diffraction were done on this type of compounds and all confirm that the spin transition of Co (II) is accompanied by a metal-metal electron transfer [7-8].

Our PBA was $[Na_{0.45}Co_{1.35}Fe(CN)_6]\cdot zH_2O$. All the studies confirmed that it is a typical PBA compound: the electron transfer takes place from Fe (II) to Co (III) and it is accompanied by the spin transition of Co. Must be specified that in PBA Co is making the transition, while in spin-crossover compounds studied here Fe is the one. We resume the process through the following reaction equation:

$$\begin{array}{ccccccc} Fe^{II}(LS) & + & Co^{III}(LS) & \rightarrow & Fe^{III}(LS) & + & Co^{II}(HS) \\ t_{2g}^{6},\ s=0 & & t_{2g}^{6},\ s=0 & & t_{2g}^{5},\ s=1/2 & & t_{2g}^{5}e_{g}^{2},\ s=3/2 \end{array}$$

We studied the pressure influence on it and compared with similar results obtained in the case of spin-crossover compounds. Also we tried to do a similar kind of experiments to this one using a new compound: $[Rb_{0.98}Mn_{1.03}Fe(CN)_6]\cdot zH_2O$. The present measurements have been achieved by performing either temperature sweeps at constant pressure or pressure sweeps at constant temperature, when it is possible. The coherence of the two sets of data is reported in terms of a phase diagram.

2. Experimental

A schematic diagram of the apparatus, which allows the simultaneous pressure, temperature and optical measurements, is shown in Fig. 1. The pressure is generated using a two-membrane pneumatic compressor, operating with helium gas. The maximum pressure obtained is the maximum pressure provided by the compressor, 1600bar. However, the device is designed for operating up to 4 kbar. It has the ability to control the rate of variation of the pressure, by using a micrometric valve. Low temperatures are easily reached by the use of cryogenic vessels (liquid nitrogen or helium) and an in-built temperature control.

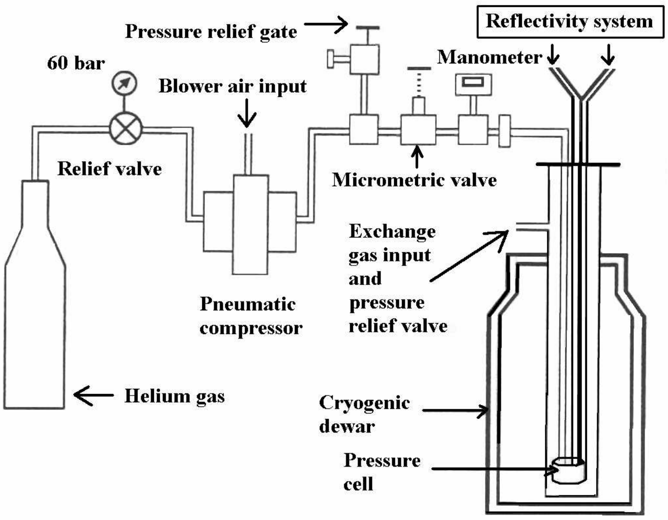

Fig. 1. The apparatus assembly from [9].

The pressure is transmitted to the sample through a high-pressure capillary tube, which is silver-welded to the pressure cell. Fig. 2 shows the pressure cell, which consists of two cylindrical blocks. Both parts are made of stainless steel and have sharp circular edges to allow the sealing using a copper ring. The optical access is provided by a conical sapphire window, sealed by an indium ring. Once the pressure has been increased, the input valve can be closed and the device maintains a quasiconstant pressure at all temperatures. It is necessary, of course, that the capillary to remain free of air condensation and for this purpose a preliminary purge of the system with helium gas is carried out.

The sample (powder in our case) is set into a small cooper sample holder inside the cell. To avoid the displacement of the sample due to the gas flow which occurs when establishing (or removing) the pressure, the sample is covered by a thin Plexiglass disc. The cryogenic system is made of a thin stainless steel tube, which houses the pressure cell and is introduced into a standard cryogenic vessel. The temperature control is achieving by using a copper block screwed to the cell and in close contact with it, through indium-coated surfaces. The copper block houses two heating resistors and a rhodium-iron thermo-element, connected to a temperature controller.

The optical detection is performed through the sapphire window and the Y-shaped optical fibre, showed in Fig. 3. The beam from the white light source passes through one part of a multibranch Y-shaped silica fibre and illuminates the sample. The reflected light is captured by the second part of the fibre and is transmitted to the other end of the fibre. Both the incident and reflected light intensities are separately measured by two photodiodes, which are connected to the input ports of the three-channel upgrade kit plugged into a temperature controller, while the temperature is recorded on the third channel. Two channels of the upgrade kit provide amplification of the signal from the corresponding photodiode.

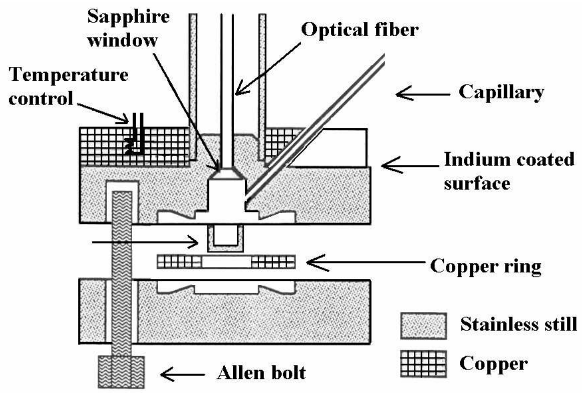

Fig. 2. A cross section of the pressure cell from [9].

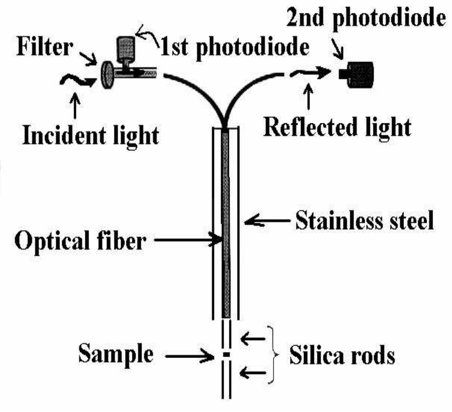

Fig. 3. Y-shaped optical fibre from [10].

A QTH (quartz tungsten halogen) lamp of 100W maximal power is the white light source. It is equipped with filters in the wavelength range from 400 to 1000nm in steps of 50nm. Periodic and non-periodic variations in the intensity of the lamp need to be corrected and an oscilloscope attached to the photodiode detects these. The periodic variations of the frequency of 100Hz are electronically averaged. To correct the non-periodic variations, the value of the reflected signal is divided by the corresponding value of the incident intensity: $I_{relative}=I_{reflected}/I_{incident}$.

3. Results and discussion

We have studied the effect of pressure on the hysteresis loops associated with the first-order spin transition of two spin-crossover compounds: pure $[Fe(btr)_2(NCS)_2]\cdot H_2O$ and diluted $[Fe_{0.52}Ni_{0.48}(btr)_2(NCS)_2]\cdot H_2O$ and compared with a PBA : $[Na_{0.45}Co_{1.35}Fe(CN)_6]\cdot zH_2O$.

The light was filtered at 550 nm in the case of spin-crossover compounds and at 700 nm in the case of PBA. The wavelength was chosen in order to have the maximum value of absorption in absorption spectra obtained with reflectivity measurements. The data are reported, assuming the existence of a linear relationship between the high spin fraction n_{HS} and the reflected intensity, in terms of I= ($I_{relative}$-I_{min}) / (I_{max}-I_{min}), where I_{min} and I_{max} were assumed to be the intensities corresponding to LS and HS state, respectively.

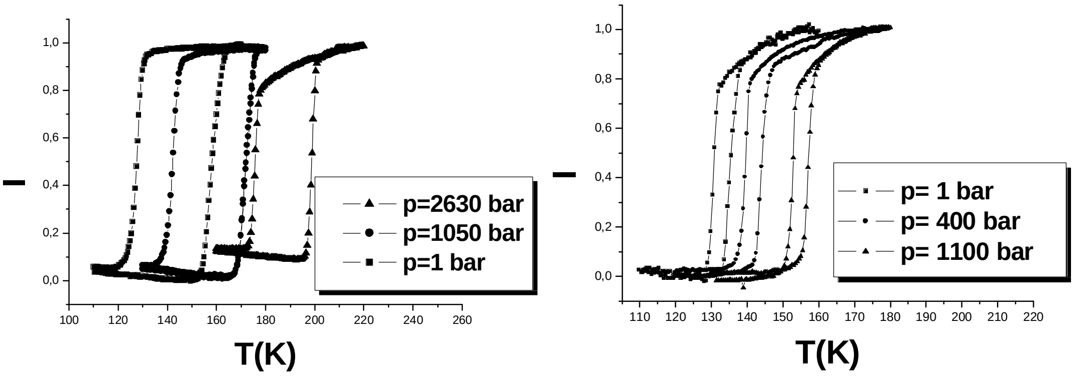

Fig. 4. Thermal hysteresis loops at constant pressure [11] [$Fe(btr)_2(NCS)_2$]·H_2O;
b. $Fe_{0.52}Ni_{0.48}(btr)_2(NCS)_2$]·$H_2O$.

The experimental data obtained for the spin-crossover compounds are shown in Figs. 4-6.

We briefly recall that pressure favours the LS state, due to its smaller volume and therefore shifts the spin equilibrium towards higher temperatures. In addition to the expected shift of the thermal transition by pressure, experimental data show also a slight decrease of the width of the histeresis. An intriguing feature in Fig. 4a is the trapezoidal shape of the hysteresis loop of the 2.6 kbar curve. We do not believe that the deviation from the squared shape relies directly to the spin transition.

These measurements lead to the (p, T) phase diagram. In the pressure range investigated, both transition temperatures T_{minus} (n_{HS} = 0.5 for the cooling mode) and T_{plus} (n_{HS} = 0.5 for the heating mode) increase linearly with p, as does the average transition temperature $T_{equ} = (T_{minus}+T_{plus})/2$, which roughly corresponds to the equilibrium temperature of the system. In every case we calculated the slope $\partial T/\partial p$ (denoted by b_{plus} and b_{minus}). The increase of b_{minus} and decrease of b_{plus} with temperature is expected, if we take into account the relation of direct proportionality between the entropy and the temperature.

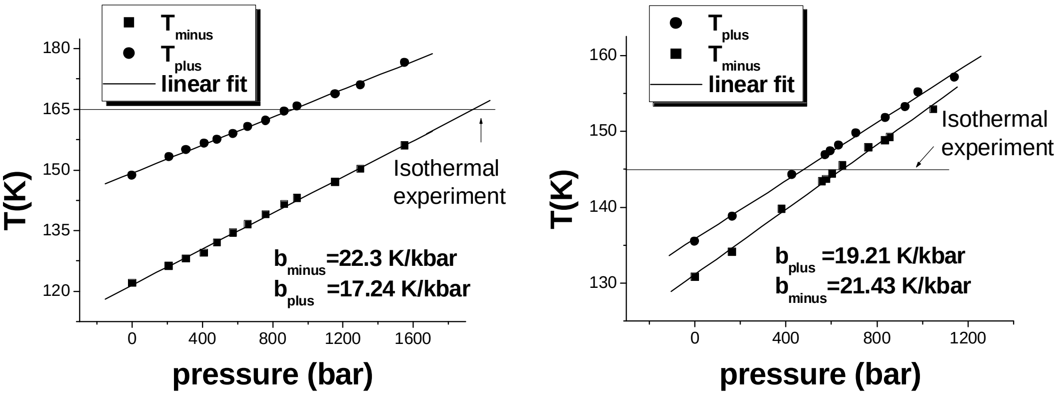

Fig. 5. Phase diagram [11] [$Fe(btr)_2(NCS)_2$]·H_2O; b. [$Fe_{0.52}Ni_{0.48}(btr)_2(NCS)_2$]·$H_2O$.

Linear extrapolation of the lines of the phase diagrams leads to the prediction that the critical pressures (pressure at which the thermal hysteresis loops would have disappeared) are higher than the maximum value of the pressure provided by the present device: $p_c \cong 5.7$ kbar for the pure compound and, respectively, $p_c \cong 2.47$ kbar for the diluted one.

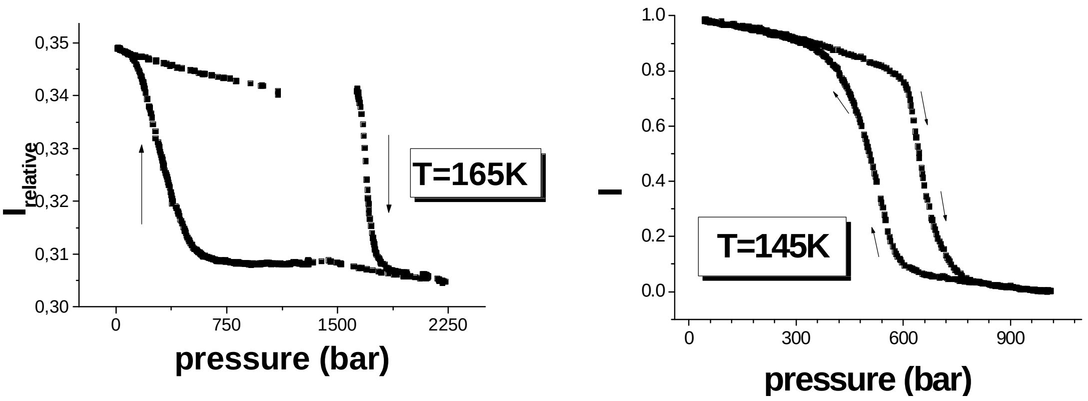

Fig. 6. Isothermal pressure loop [11] $[Fe(btr)_2(NCS)_2]\cdot H_2O$; b. $[Fe_{0.52}Ni_{0.48}(btr)_2(NCS)_2]\cdot H_2O$.

Starting from these phase diagrams we obtained isothermal pressure loops (see Fig. 6). If we take into account that the width of the hysteresis cycles is bigger in the case of the pure compound (due to the stronger cooperativity), we are able to explain why it is harder to obtain pressure loops in the case of this compound.

In the case of the typical PBA, $[Na_{0.45}Co_{1.35}Fe(CN)_6]\cdot zH_2O$, we did the same kind of analysis (see Fig. 7). We obtained the expected results: the transition temperature increases when the pressure is increased and the width of the hysteresis loops is decreasing with pressure. We obtained the same behaviour of the slopes b_{plus} and b_{minus} with temperature and the linear extrapolation suggests also a high critical pressure: $p_c \cong 5.1$ kbar.

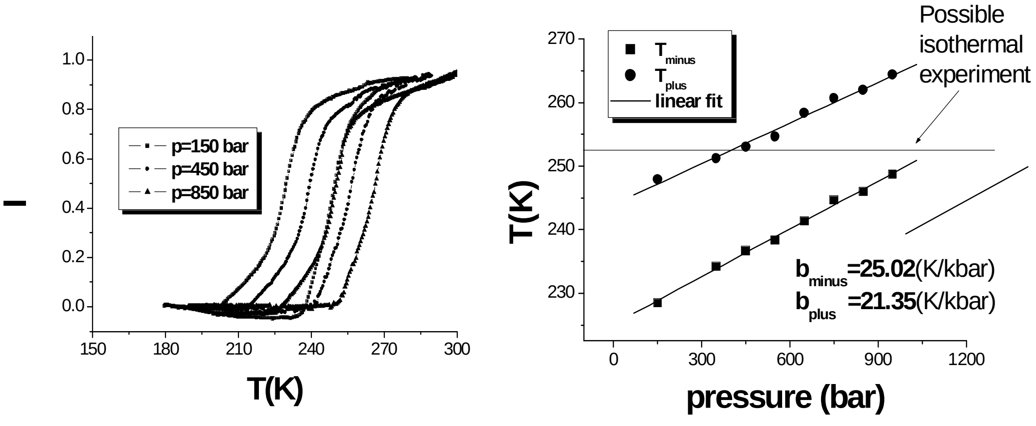

Fig. 7. $[Na_{0.45}Co_{1.35}Fe(CN)_6]\cdot zH_2O$ a. Thermal hysteresis loops; b. Phase diagram.

Our last study was made on a new compound: $[Rb_{0.98}Mn_{1.03}Fe(CN)_6)]\cdot zH_2O$. First, we thought that this compound is also a PBA in which takes place a spin transition accompanied by a charge transfer between Mn and Fe. However, Mössbauer measurements show only the presence of low spin Fe (II) at all temperatures. Then the charge transfer does not take place on this sample. The existence of a spin transition on the Mn still remains under study. We assume for the present compound that the observed first-order structural phase transition is driven by a cooperative Jahn-Teller effect.

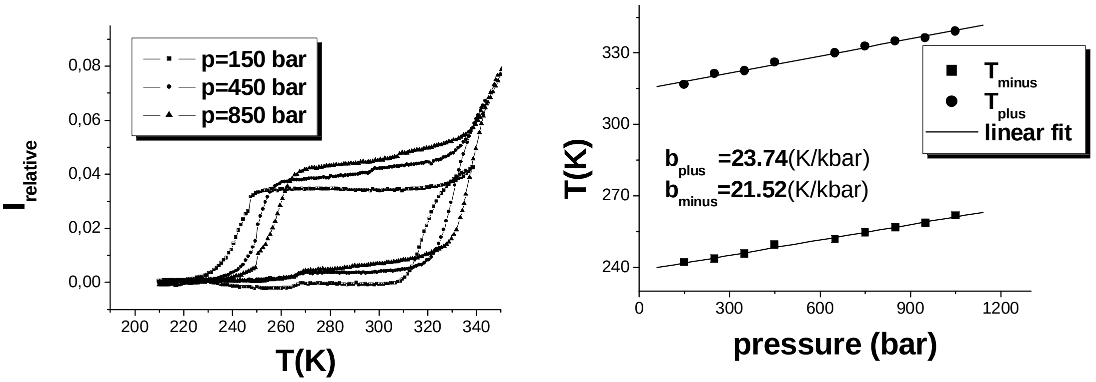

Fig. 8. $[Rb_{0.98}Mn_{1.03}Fe(CN)_6)]\cdot zH_2O$ a. Thermal hysteresis loops; b. Phase diagram.

Fig. 8 shows the results related to the effect of the pressure on this compound. In Fig. 8a we can easily observe that the thermal hysteresis widths are bigger than that of Na-PBA. So, we expect to obtain a high critical pressure p_c. The thermal behaviour of b_{minus} and b_{plus} confirms that p_c cannot be reached. The obtained unusual form of thermal hysteresis loops at high pressures could be related to the optical detection, which characterizes only the surface of the sample. Indeed, the magnetic measurements do not show any increase of the signal at high temperatures (see Fig. 9). Possible explanations of the enhancement of the reflected signal are: (i) effect of removing of water molecules at high temperatures; (ii) effect of shift of the optical band with temperature. Due to the fact that PBA samples are dark-brown, the intensity of the reflected signal is of the same order of magnitude with the experimental noise, which can be an origin for the unusual form of the loops.

However, from the theoretical point of view the study on the influence of the pressure on such systems is much complicated than the influence of light and temperature. Pressure acts on the spin state, hence change the electronic state of atoms, but also acts on the lattice. Even at the moment there are no models, which take into account the phonons, the theory still confirms the experimental data.

In spin transition systems, one of the most frequently used models is the Ising-like model, in its mean field version [12]. Accordingly, the first order transition occurs only above a threshold value of the interaction parameter given by: $q\ J_c= k\ T_{equ}= 2\Delta/\ \ln g$, in which q is the coordinence and J interaction parameter. Taking into account that the critical energy gap is given by $\Delta_c= \Delta(0)+ p_c\ |\Delta V|$, we obtain: $p_c= \Delta S/2\Delta V\cdot[qJ/k\text{-}T_{equ}(p=0)]$, where T_{equ}, p_c and $\Delta V/\Delta S= \partial T/\partial p$ are experimentally determined. From the obtained p_c values, we found for the interaction parameter qJ: 366.158 K, 362.825K and 470.036K corresponding respectively with samples (1), (2) and (3). The relevant parameter allowing us to compare the degree of cooperativity is $x=kT_{equ}/qJ$, which gives for the three samples the values: 0.384, 0.723 and 0.496, respectively. In contrast with the obtained absolute values for the cooperativity, the parameter x is in very good agreement with the behaviour of the width of the experimental hysteresis loops (see Fig. 10).

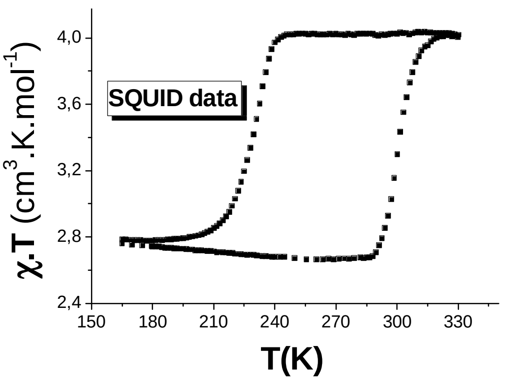

Fig. 9. Magnetic measurements for Rb-PBA.

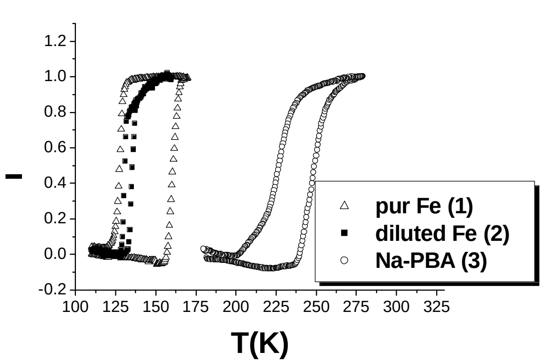

Fig. 10. Thermal hysteresis loops at p= 1 bar.

4. Conclusions

The effects of the pressure on spin crossover compounds and Prussian blue analogues are easily characterized by optical measurements. The phase transition and the temperature at which we obtained the pressure hysteresis loop were indicated. Considering that $\partial T/\partial p$ is defined as $\Delta V/\Delta S$ [1], then a possible study can be carried out combining this type of measurements with X-ray diffraction or calorimetric measurements. An interesting goal for the future would be also a combination between pressure device and photo excitation techniques, when a LIPH (Light Induced Pressure Hysteresis) is expected. The study of the combined effects of light, temperature and pressure will improve our knowledge of these photosensitive materials and will facilitate the development of future applications.

Acknowledgements

We are indebted to Prof. K. Hashimoto (Research Center for Advanced Science and Technology, the University of Tokyo) for supplying the PBA samples. A. Sava would like to thank Socrates Program and CNRS for their financial support during her stay in Versailles.

References

[1] O. Kahn, "Molecular magnetism", VCH New York, (1995).
[2] O. Kahn, J. Kröber, C. Jay, Adv. Mat. **4**, 718 (1992).
[3] P. Gűtlich, A. Hauser, H. Spiering, Angew. Chem. Int. Ed. Engl. **33**, 2024 (1994).
[4] A. Desaix, O. Roubeau, J. Jeftic, J. G. Haasnoot, K. Boukheddaden, E. Codjovi, J. Linares, M. Noguès, F. Varret, Eur. Phys. J. B **6**, 183 (1998).
[5] C. Enachescu, J. Linares, F. Varret, J. Phys. Condens. Matter **13**, 2481 (2001).
[6] A. Bleuzen, C. Lomenech, V. Escax, F. Villain, A. F. Varret, C. Cartier dit Moulin, M. Verdaguer, J. Am. Chem. Soc. **122**, 6648 (2000).
[7] C. Cartier dit Moulin, F. Villain, A. Bleuzen, M. –A. Arrio, P. Sainctavit, C. Lomenech, V. Escax, F. audelet, E. Dartyge, J. J. Gallet, M. Verdaguer, J. Am. Chem. Soc. **122**, 6653 (2000).
[8] V. Escax, A. Bleuzen, C. Cartier dit Moulin, F. Villain, A. Goujon, F. Varret, M. Verdaguer, J. Am. Chem. Soc. **123**, 12536 (2001).
[9] J. Jeftic, N. Menendezk, A. Wack, E. Codjovi, J. Linares, A. Goujon, G. Hamel, S. Klotz, G. Syfosse, F. Varret, Meas. Sci. Technol. **10**, 1059 (1999).
[10] W. Morscheidt, J. Jefic, E. Codjovi, J. Linares, A. Bousseksou, H. Constant-Machado, F. Varret, Meas. Sci. Technol. **9**, 1311 (1998).
[11] E. Codjovi, N. Menendez, J. Jeftic, F. Varret, C. R. Acad. Sci. Paris, Chimie/ Chemistry **4**, 181 (2001).
[12] K. Boukheddaden, I. Sheto, B. Hôo, F. Varret, Phys. Rev. B. **62**(22), 14796 (2000).